MOLECULAR DYNAMICS SIMULATION OF Ca^{2+} HYDRATION AND THE OPTICAL RESPONSE OF CLUSTERED WATER

JASON BYRD, FERNANDO VILA, YOSHINARI TAKIMOTO, AND JOHN REHR

1. Introduction

Ion hydrates in polar solutions is a rich and multi-disipline topic. Examples can be found in molecular biology topics such as nerve signal transfer, electrolyte transport, nutrient transport through cell walls, and inter-cell communication. Industrial applications such as toxic chemical studies and treament in ground water, and polar solvent hydration of surfaces. Examples of these are UO_2 and U_2 hydration in ground water, and MgO surface interaction with polar solvents. The investigation of Ion hydrates directly ties with the properties of bulk and cluster water systems. To understand hydration of materials, the structure of different water systems must be understood. In addition, theoretical calculations of cluster and bulk water beahvior is not well understood.

The hydration of Ca^{2+} and $Ca^{2+}Cl_2$ is a well known phenomina, and so makes an excelent material for the testing of theoretical models. Well tested quantities include first shell coordination numbers and radial distribution functions. We show that the use of classical molecular dynamic calculations with an single point charge model for water give good agreement with experimental reports by implimenting the Groningen Machine for Chemical Simulations (GROMACS) package.

Investigation of cluster water in the soft UV range is a difficult experimental and theoretical system to obtain. Edge effects and cluster sizes dominate any calculations, and internal structure greatly shifts any results obtained. The soft UV spectrum of clustered water is investigated using real time-time dependant functional theory calculations with the Spanish Initiative for Electronic Simulations with Thousands of Atoms (SIESTA). It is shown that with an appropriate basis set the soft UV spectrum of cluster water can be accurately calculated. From this, it is possible to calculate the soft UV spectrum of many other systems that interact or are members of clustered water systems.

2. Classical Molecular Dynamic Calculation Methods and Results

The solvation structure of Ca^{2+} in a water solvent was calculated using the GROMACS classical molecular dynamic routines (1; 2), using the GROMOS96 43a1 force field to calculate the trajectories of the system. Initial configurations were calculated by a random placement of water molecules about the Ca^{2+} atom (centered in the calculation box initially). Any overlapping molecules are removed from the system, then energy minimization is performed on the system to relax any bad Potential. A positional relaxation calculation is performed on the full system, to obtain an optimized configuration of solvents and the ion. This positional relaxation reduces the time needed to reach equilibrium with the full classical molecular dynamics run, with very little computational time used.

Date: Fall-2005.
The first author was funded by an NSF REU grant.

The full classical molecular dynamics calculation was performed over a 1.2 ns time interval, with snapshots taken every 0.002 ps. The interaction potentials used in the dynamics calculation uses the Lennard-Jones repulsive and dispersive potential

$$V_{ij}(r) = \frac{A_{ij}}{r_{ij}^{12}} - \frac{B_{ij}}{r_{ij}^{6}}. \tag{1}$$

Water molecules are represented using the SPC potential proposed by Berendsen *et al.* (3), where the partial charges for the oxygen is $-0.82E$ and for the hydrogen is $0.41e$. The ion-solvent and solvent-solvent interactions are described by a Coulomb-Lennard Jones potential of the form

$$V_(r) = \sum_{i \neq j} (\frac{Q_{ij}}{r_{ij}} + \frac{A_{ij}}{r_{ij}^{12}} - \frac{B_{ij}}{r_{ij}^{6}}). \tag{2}$$

The behavior of the solvent near the Ca^{2+} ion can be described by two radial distribution functions (or RDF) for the water Oxygen and Hydrogen (O_w and H_W respectively). These RDF calculations consist of a normalized average radial density function $\langle \rho(r) \rangle$, so that the RDF $g(r)$ is defined (4) as

$$g(r) = \frac{\langle \rho(r) \rangle}{\langle \rho(r_{local}) \rangle} = \frac{1}{\langle \rho(r_{local}) \rangle} \frac{1}{N_i} \sum_{k \in i}^{N_i} \sum_{l \in j}^{N_j} \frac{\delta(r-r)}{4\pi r^2}. \tag{3}$$

Where r_{local} is half the box length and $\langle \rho(r_{local}) \rangle$ represents the effective density of the solvent box at equilibrium.

This first maximum of $g_{CaO}(r)$ is shown in Figure 1 to be 2.47±0.05Å, which corresponds to the mean radius of the first hydration sphere (HS). Other reported theoretical results for the first hydration sphere radius are 2.67Å(5) using classical molecular dynamics and 2.47Å, 2.37Å and 2.45 Å(6) (calculated with classical molecular dynamics and QM/MD respectively).

Experimental results for $Ca^{2+} - H_2O$ hydration include 2.46 Å with X-ray diffraction (7), 2.40 Å using neutron diffraction (8) and 2.46Å with EXAFS and LAXS (9). Discrepancies in the hydration shell values can be explained by differences in concentration(5) and interaction effects from $Ca^{2+}Cl_2$ salts in the experiments. Another factor that effects simulated results is the underestimation of ion-solvent and solvent-solvent interadtions by the SPC model of water (10). This underestimation by will result in an over estimate the distance between ions and the solvent to give the peak shift seen.

In addition to obtaining solvent mass distribution about the ion with the RDF, the shell coordination number n can be obtained as

$$n = 4\pi \langle \rho(r_{local}) \rangle \int_0^{r_{min}} dr g(r) r^2, \tag{4}$$

where r_{min} is the location of the RDF minima after the shell in question. The first hydration shell of Ca^{2+} in water consists of 6 water molecules in the gas phase, and 8 to 9 in the condensed phase. Integration of Eqn. 4 for the $Ca^{2+} - O_w$ RDF shown in Figure 1 yields a coordination number of 7.44, which is in good agreement with the experimental results of 7.3 (8) and 8 (8; 9).

3. Optical Response of water

The calculation of frequency-dependent optical response of liquid water is done using real time-time dependent density functional theory (RT-TDDFT) as implemented by Tsolakidis *et al.* (11) using SIESTA (12). Briefly, SIESTA is a DFT program that uses a local

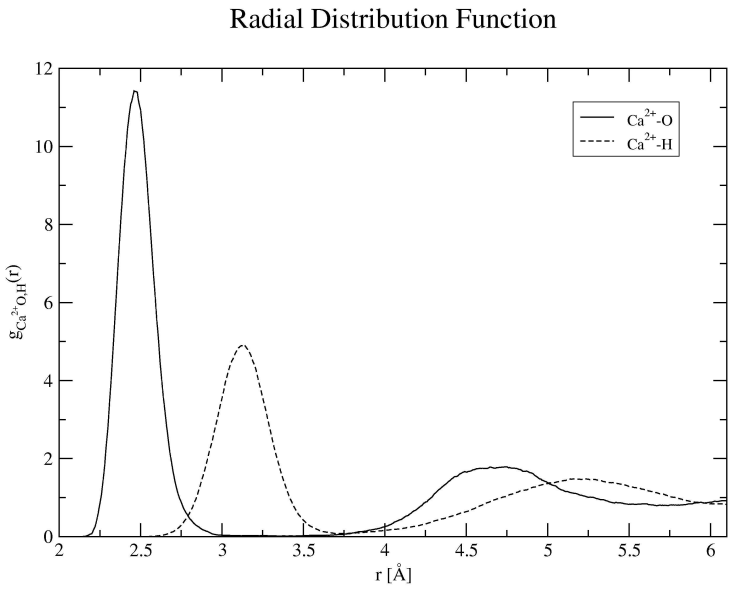

Figure 1: $Ca^{2+} - O_w$ and $Ca^{2+} - H_w$ RDF results

basis and optimized for large order systems. SIESTA is attractive to this problem because it uses confined (strictly zero beyond the cutoff radius) numerical atomic orbitals (NAO), which are built with the eigenstates of atomic pseudopotentials. This use of confined NAOs and localized Wannier-like electron wave functions cuts the computational and storage costs considerably, and allows the program to scale linearly with system size(12; 11).

We calculate the linear response of the system to an external electric field E by introducting a perturbation Hamiltonian $\delta H = -E \cdot x;\ E$. Once selfconsistency has been reached, the electric field is turned off ($t = 0$) and the time dependence of the system is calculated using the Hamiltonian

$$H = -\frac{1}{2}\nabla^2 + V_{ext}(r,t) + \int dr'(\frac{\rho(r',t)}{|r-r'|}) + V_{xc}[\rho](r,t). \tag{5}$$

The calculation of the exchange-correlation (xc) potential $V_{xc}[\rho](r,t)$ is performed using the adiabatic local density approximation (ALDA), which gives

$$V_{xc}[\rho](r,t) = \frac{\delta E_{xc}^{LDA}[\rho_t]}{\delta \rho_t(r)} = V_{xc}^{LDA}[\rho_t](r,t) \tag{6}$$

where $E_{xc}^{LDA}[\rho_t]$ represents the exchange-correlation energy of the homogeneous electron gas(13) calculated with the instantaneous density ρ_+.

The dipole moment of the system $D(t)$ is calculated at each time step and the frequency-dependant response is found by a Fourier transform

$$D(\omega) = \int_0^\infty dt e^{(i\omega - \delta)t)} D(t) \tag{7}$$

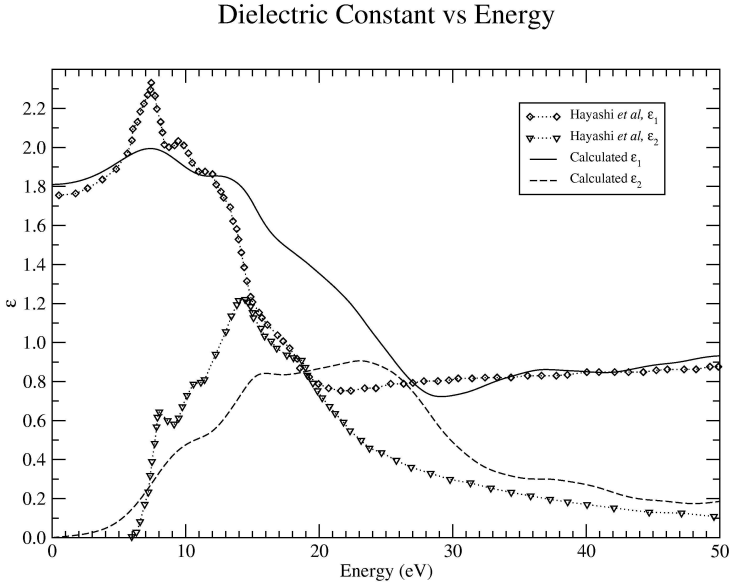

Figure 2: Real (ϵ_1) and imaginary (ϵ_2) parts of the dielectric constant of $(H_2O)_{44}$ water.

where δ is a damping factor introduced to account for broadening, and effectively sets the minimum width of the peaks in the imaginary response. Thus to linear order the polarizability $\alpha(\omega) = D(\omega)/E(\omega)$ or

$$Im\ \alpha(\omega) = \omega \frac{Re\ D(\omega)}{E} \tag{8}$$

with $E(t) = E\theta(-t)$. After calculating the response along different axes, the average linear polarizability is one-third the trace of the polarizability tensor such that $\langle\alpha\rangle = Tr\{\alpha_{ij}(\omega)\}$. The dielectric response of the system as a function of frequency. This can be obtained from

$$\epsilon(\omega) = 1 + 4\pi\alpha(\omega)/V_{clust} \tag{9}$$

where V_{clust} is the electron volume of the system. The quantity $\alpha(\omega)$ is calculated using Eqn. 8, and the relation $Im\ \alpha(\omega) = \omega\frac{Re\ D(\omega)}{E}$ to arrive at

$$\epsilon(\omega) = 1 + 4\pi\omega \frac{(Im\ D(\omega) + iRe\ D(\omega))}{E\theta(-t)V_{clust}},\ \text{or} \tag{10}$$

$$\epsilon_1(\omega) = 1 + 4\pi\omega \frac{Im\ D(\omega)}{E\theta(-t)V_{clust}},\ \epsilon_2(\omega) = 4\pi\omega \frac{iRe\ D(\omega)}{E\theta(-t)V_{clust}} \tag{11}$$

The optical response was calculated for liquid water in an equilibrium state with a molecular density of $0.034 molec/\text{Å}^3$. This was calculated using the molecular mechanic simulations discussed above. Problems with intrinsic dipole moments to the water clusters was avoided by doing a Monte Carlo sample of the bulk water system, and choosing the clusters with the most optimal configuration (see Appendix A for detais).

The real and imaginary part of the dielectric constat are shown in Figure 2. Hayashi *et al.*'s results for $\epsilon(\omega)$ (15) show that while our calculated $\epsilon(\omega)$ has both the correct shape and

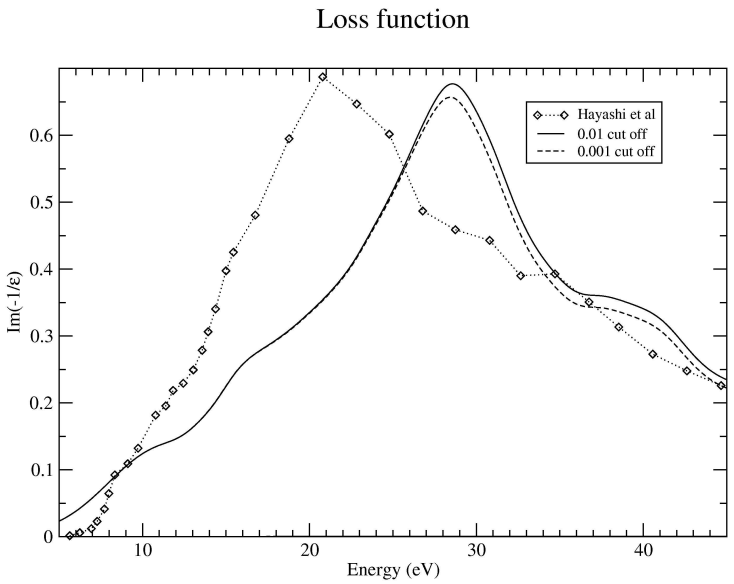

Figure 3: Calculated loss function $Im(-1/\epsilon(\omega))$ compared to experiment (14) for liquid water.

comparable magnitudes, there is a distinct shift of the peaks towards higher energy levels after 15 eV. This can be clear seen by calculating the loss function

$$Im(-\frac{1}{\epsilon(\omega)}) = \frac{\epsilon_2}{\epsilon_1^2 + \epsilon_2^2}, \tag{12}$$

which is shown in Figure 3 against data from Hayashi *et al.* (14). It is clear that there is a significant shift in peak values towards higher energy levels. The shift towards higher energies in both the loss function and dielectric constant are strong indicators of issues with the methods used to calculate the electric response of the clusters. It has bene shown by Cabral do Couto*et al.* (16) that insufficient basis sets will cause a shift towards higher energies.

4. Conclusions

We show that with GROMACS, we can accurately compute the molecular behavior of solvents near ions. Using an apropriate basis set, it is also possible to accurately describe the electronic behavior of water. With an improved basis set, edge effects on water clusters and the soft UV structure of water interacting with other ions.

Appendix A. Optimal Configuration Algorithm

The optimal configuration of the sub-group of the calculated equilibrium liquid water system was calculated by forming a sphere about some arbitrary point in the box, then the sub-group's dipole moment was calculated using the formula $P = \sum r_i q_i$. The radius of the sphere chosen was picked by using the molecular density $0.034 \text{molec} \text{Å}^3$ and a general requirement of molecules per sub-group. This intrinsic dipole moment was used to determine the optimal structures by defining a dipole maximum cutoff, and only keeping structures in this subset that have the lowest possible dipole moment.

Because of the size of the system and number of molecules, it is clear that a statistical sampling of sub-group center coordinates is advantageous when searching for a specific cutoff for the sub-group dipole moment. This is done via Monte Carlo simulation, where the sub-group center coordinate is randomly generated, followed by the calculation of the dipole moment. Analysis of this raw information is done efficiently by using the hash capabilities in Perl. Following the calculation of the dipole moment for each sub-group, a hash of each molecule that is a member of the sub-group is saved and keyed against the Monte Carlo loop index. A hash is also built of all the Monte Carlo look indexes using the scalar dipole moment of each index as a key, this is important because after the Monte Carlo run is finished it is a simple sort and loop over keys to the dipole hash to get the information needed.

Overview of the sub-group selection algorithm.

```
### do random seed across the box
  srand( time() ^ ($$ + ($$ << 15)) );
  for ($ri = 1; $ri < 7000; $ri++) {
    $dipx = 0.000; $dipy = 0.000; $dipz = 0.000;
 #create random center
    $cx = rand 20;  $cx-=10.000;
    $cy = rand 20;  $cy-=10.000;
    $cz = rand 20;  $cz-=10.000;
 #loop over each atom in the file
    for ($i = 0; $i < scalar(@x); $i++) {
 #keep only oxygen
      if ($Atype[$i] =~ /$Asearch/g) {
 #r scalar length to i'th O atom
        $r=sqrt(abs(($x[$i]-$cx)**2+($y[$i]-$cy)**2+($z[$i]-$cz)**2));
 #calculate dipole contribution of the $ith molecule
        if ($r < $rcutoff) {
```

Here calculate the dipole moment of the system.

```
 #hash of atoms per $ri run
          $atoms{$ri} = [] unless exists $atoms{$ri};
          push @{$atoms{$ri}}, $i;
        }
      }
    }
 #hash of dipole moments vs index
    $nr = sqrt(abs( $dipx**2 + $dipy**2 + $dipz**2 ))*$scale;
 #keep the dipoles around
    $mydipolehash{$nr} = [] unless exists $mydipolehash{$nr};
    push @{$mydipolehash{$nr}}, $ri;
 #save index of each good dipole system, or skip to next run
    if (scalar sort @{$atoms{$ri}}) {
      if ($nr < 2.5) { push(@risk,$ri);} else { next; }
    }
 #hash of cx,cy,cz vs index
    $coordinatehash{$ri} = [] unless exists $coordinatehash{$ri};
    push @{$coordinatehash{$ri}}, ($cx,$cy,$cz);
  }
```

References

[1] H. Berendsen, D. van der Spoel, R. van Drunen: *Comp. Phys. Comm.* **91** (1995) 43
[2] E. Lindahl, B. Hess, D. van der Spoel: *J. Mol. Mod.* **7** (2001) 306
[3] H. J. C. Berendsen, J. P. M. Postma, W. F. van Gusteren, J. Hermans: *Intermolecular Forces* (1981)
[4] D. van der Spoel, E. Lindahl, B. Hess, A. R. van Buuren, E. Apol, P. J. Meulenhoff, D. P. Tieleman, A. L. T. M. Sijbers, K. A. Feenstra, R. van Drunen, H. J. C. Berensden: *www.gromacs.org* (2005)
[5] K. Bujnicka, E. Hawlicka: *J. Mol. Liquids* **125** (2006) 151
[6] A. Tongraar, K. Liedl, B. M. Rode: *J. Phys. Chem. A* **101** (1997) 6299
[7] T. Megyes, T. Grosza, T. Radnai, I. Bako, G. Palinkas: *J. Phys. Chem. A* **108** (2004) 7261
[8] Y. S. Badyal, A. C. Barnes, G. J. Cuello, J. M. Simonson: *J. Phys. Chem. A* **108** (2004) 11819
[9] F. Jalilehvand, D. Spøangberg, P. Lindqvist-Reis, K. Hermansson, I. Persson, M. Sandström: *J. Am. Chem. Soc.* **123** (2001) 431
[10] E. Howlicka, D. Swiatla-Wojcik: *J. Phys. Chem. A* **106** (2002) 1336
[11] A. Tsolakidis, D. Sánchez-Portal, R. M. Martin: *Phys. Rev. B* **66** (2002) 235416 1
[12] J. M. Soler, E. Artacho, J. D. Gale, A. Garcia, J. Junquera, P. Ordejón, D. Sánchez-Portal: *J. Phys.: Condens. Matter* **14** (2002) 2745
[13] D. M. Ceperley, B. J. Alder: *Phys. Rev. Lett.* **45** (1980) 566
[14] H. Hayashi, N. Watanabe, Y. Udagawa: *J. Chem. Phys.* **108** (1998) 823
[15] H. Hayashi, N. Watanabe, C.-C. Kao: *PNAS* **97** (2000) 6264
[16] P. Cabral do Couto, R. C. Guedes, B. J. Costa Cabral: *Brazilian Journal of Physics* **34** (2004) 42

E-mail address: madbosun@gmail.com

Institute for Nuclear Theory, University of Washington